HHS Public Access

Author manuscript

J Neural Eng. Author manuscript; available in PMC 2023 October 31.

Published in final edited form as:

J Neural Eng. ; 19(5): . doi:10.1088/1741-2552/ac9a00.

Spinal stimulation for motor rehabilitation immediately modulates nociceptive transmission

Maria F. Bandres[a,e], **Jefferson L. Gomes**[a], **Jacob G. McPherson**[a,b,c,d,e]

[a]Program in Physical Therapy, Washington University School of Medicine in St. Louis

[b]Department of Anesthesiology, Washington University School of Medicine in St. Louis

[c]Washington University Pain Center, Washington University School of Medicine in St. Louis

[d]Program in Neuroscience; Washington University School of Medicine in St. Louis

[e]Department of Biomedical Engineering; Washington University in St. Louis

Abstract

Objective: Spinal cord injury (SCI) often results in debilitating movement impairments and neuropathic pain. Electrical stimulation of spinal neurons holds considerable promise both for enhancing neural transmission in weakened motor pathways and for reducing neural transmission in overactive nociceptive pathways. However, spinal stimulation paradigms currently under development for individuals living with SCI continue overwhelmingly to be developed in the context of motor rehabilitation alone. The objective of this study is to test the hypothesis that motor-targeted spinal stimulation simultaneously modulates spinal nociceptive transmission.

Approach: We characterized the neuromodulatory actions of motor-targeted intraspinal microstimulation (ISMS) on the firing dynamics of large populations of discrete nociceptive specific and wide dynamic range neurons. Neurons were accessed via dense microelectrode arrays implanted *in vivo* into lumbar enlargement of rats. Nociceptive and non-nociceptive cutaneous transmission was induced before, during, and after ISMS by mechanically probing the L5 dermatome.

Main results: Our primary findings are that (1) sub-motor threshold ISMS delivered to spinal motor pools immediately modulates concurrent nociceptive transmission; (2) the magnitude of anti-nociceptive effects increases with longer durations of ISMS, including robust carryover effects; (3) the majority of all identified nociceptive-specific and wide dynamic range neurons exhibit firing rate reductions after only 10 min of ISMS; and (4) ISMS does not increase spinal responsiveness to non-nociceptive cutaneous transmission. These results lead to the conclusion that ISMS parameterized to enhance motor output results in an overall net decrease in spinal nociceptive transmission.

Corresponding author: Jacob G. McPherson, mcpherson.jacob@wustl.edu, Program in Physical Therapy, Washington University School of Medicine, 4444 Forest Park Avenue, Suite 1101, St. Louis, MO 63108.

Author Contributions: JGM designed and oversaw the research; MFB, JLG, and JGM performed the research; MFB and JGM analyzed the data; MFB, JLG, and JGM interpreted the data; MFB and JGM wrote and edited the paper.

Competing Interest Statement: The authors declare no competing financial interests.

Significance: These results suggest that ISMS may hold translational potential for neuropathic pain-related applications and that it may be uniquely suited to delivering multi-modal therapeutic benefits for individuals living with SCI.

Keywords

spinal cord; spinal cord injury; spinal stimulation; neuromodulation; motor; neuropathic pain; rehabilitation; neural plasticity

Introduction

Electrical stimulation of spinal circuits below a spinal cord injury (SCI) is an emerging approach to recruit damaged yet spared neurons to enhance voluntary motor output (1–7). When combined with physical therapy, spinal stimulation holds considerable promise for facilitating functionally meaningful therapeutic gains. However, motor impairments are far from the only consequence of inappropriate SCI-related neural transmission for which spinal stimulation may be particularly efficacious. For example, spinal responses to sensory feedback often become pathologically increased below an SCI, contributing to neuropathic pain (SCI-NP) in ~70% of individuals living with incomplete SCI (8).

Electrical stimulation of spinal circuits is also an emerging approach to manage enigmatic chronic pain syndromes such as persistent spinal pain syndrome, complex regional pain syndrome, neuropathic pain syndromes, and ischemic pain syndromes (9–12). The ability of spinal stimulation to reduce pathologic neural transmission associated with SCI-NP has only been preliminarily investigated (13). However, many of the therapeutic benefits of spinal stimulation for SCI-related motor impairments derive from a neural mechanism that is also presumed to underlie many of the benefits of paresthesia-based spinal stimulation for neuropathic pain. Namely, recruitment of low-threshold, non-nociceptive sensory afferent fibers and interneurons (14–19).

The putative mechanistic overlap between spinal stimulation parameterized to enhance motor output and spinal stimulation parameterized to ameliorate neuropathic pain leads to the hypothesis that spinal stimulation for motor rehabilitation will have simultaneous, albeit off-target, effects on nociceptive transmission. If so, it also raises the intriguing possibility that spinal stimulation paradigms could be developed specifically to provide multi-modal therapeutic benefits (rather than the domain-specific parameterizations developed to date). However, the potential effects of ‘motor-targeted’ spinal stimulation on nociceptive transmission have yet to be directly characterized.

Here, we test the hypothesis that motor-targeted spinal stimulation will simultaneously modulate spinal nociceptive transmission. Specifically, we characterize the neuromodulatory actions of motor-targeted intraspinal microstimulation (ISMS) *in vivo* in rats using dense microelectrode arrays implanted into the spinal cord. This approach allows us to simultaneously record from large populations of discrete neurons spanning sensory and motor regions of the lumbar gray matter. It also allows neurons to be functionally classified as either nociceptive specific or wide dynamic range to infer the potential behavioral implications of ISMS. We found immediate and in cases persistent modulation

of nociceptive transmission by motor-targeted ISMS. Contrary to our expectation, ISMS did not robustly modulate non-nociceptive cutaneous transmission. These observations reveal the potential of ISMS to deliver contextually relevant multi-modal therapeutic benefits while also underscoring the importance of considering off-target effects when developing new spinal stimulation paradigms.

Materials and Methods

We characterized the impact of motor-targeted ISMS on nociceptive and non-nociceptive transmission in nociceptive specific (NS) neurons and wide dynamic range (WDR) neurons across 14 adult male Sprague-Dawley rats (~250–500 g). All procedures were approved by the Institutional Animal Care and Usage Committees of Florida International University and Washington University in St. Louis. The surgical, experimental, and analytical approaches utilized here have been previously detailed (1, 20, 21); a brief account of each is provided below.

Surgical Procedures

Anesthesia was induced using inhaled isoflurane (~3–4% in O_2, flow rate: ~0.9–1.6 L/min). Urethane (1.2 g/Kg i.p.) was then administered for anesthetic maintenance, with boosts as necessary (0.2 g/Kg i.p.). We selected urethane because it preserves the spinal excitability required to activate spinal nociceptive pathways (20). After achieving a deep, surgical plane of anesthesia, a ~5 cm midline skin incision was made over the vertebral column. The exposed subcutaneous tissue and musculature were retracted and a T13-L2 laminectomy was performed under magnification (Leica Microsystems, Inc). Body temperature, heart rate, respiration rate, and SpO_2 were monitored continuously (Kent Scientific, Inc.). Temperature was controlled by heating pads and lactated ringer solution was administered subcutaneously every 2 hrs to prevent dehydration.

Animals were then transferred to an anti-vibration air table (Kinetic Systems, Inc.) enclosed by a Faraday cage. Vertebrae rostral and caudal to the laminectomy were secured via locking forceps to a custom, multi-degree-of-freedom fixation frame. The animal's abdomen was then elevated to attenuate upward and downward movements of the chest cavity or spinal cord during respiratory cycles. The spinal meninges were incised rostro-caudally, reflected, and the exposed spinal cord was bathed in homeothermic ringer solution.

Electrode implantation and electrophysiological recordings

We used therapeutic intraspinal microstimulation (ISMS) as our platform for characterizing the potential impact of motor-targeted spinal stimulation on nociceptive transmission. ISMS and extracellular neural recordings from the gray matter of the lumbar enlargement were realized using 32-channel microelectrode arrays (NeuroNexus Inc.) custom electrodeposited with activated platinum-iridium (Platinum Group Coatings, Inc.). The arrays had two shanks that each contained 16 discrete, vertically aligned electrodes (electrode area: 177 μm^2; inter-electrode spacing: 100 μm; impedance: 4–10 KΩ). Prior to implantation, microelectrode arrays were coated with 1,1'-Dioctadecyl-3,3,3',3'-tetramethylindocarbocyanine perchlorate (Sigma-Aldrich, Inc.) to aid post-mortem histological localization of the electrode tracks

(Fig. 1a). Microelectrode arrays were mated via Omnetics nano connectors to a Ripple Nano2+Stim headstage and Grapevine data acquisition/stimulation system (Ripple Neuro, Inc.). The headstage was securely fastened to a four-axis motorized micromanipulator with submicron resolution (Siskiyou Corp.).

For implantation into the spinal cord, the electrode array was oriented perpendicular to the midline and positioned coarsely over the L5 dorsal root entry zone under high magnification. Precise intraoperative localization of the L5 dorsal root entry zone was aided by monitoring dorsal root potentials during mechanical stimulation of the glabrous skin of the plantar surface of the hindpaw, as evidenced by real-time visualization of multiunit neural activity and by patching the multiunit neural waveforms through a high-fidelity electrophysiology audio amplifier (A-M Systems, Inc.). If clearly correlated dorsal root potentials were not visible when probing the desired receptive field, the microelectrode array was moved to a new location. When a site was identified such that dorsal root potentials were synchronous with receptive field mapping, insertion of the microelectrode array commenced.

The microelectrode array was inserted slowly into the spinal cord, in increments of ~25 μm, to minimize shear and planar stress on the neural tissue. When the deepest electrodes of the array reached the dorsal-most border of the deep dorsal horn (~400–500 μm deep to the surface of the spinal cold), we again mapped the L5 dermatome. If the receptive field remained appropriate, we proceeded to fully implant the electrode (with the deepest electrodes targeting motor pools of the ventral horn, ~1600–1800+ μm deep to the surface of the spinal cord; Fig. 1a). Once fully implanted, the L5 dermatome was again mapped. If the most sensitive areas of the receptive field had shifted substantially, for example to the hairy skin bordering the foot, the microelectrode array was retracted and reimplanted. Electrodes were otherwise not moved after full implantation.

We next determined resting motor threshold in each animal. Single pulses of charge-balanced current (cathode leading, 200 μs/phase, 0 s inter-phase interval) were delivered to electrodes located in the ventral horn with increasing current intensities until a muscle twitch was detected in the L5 myotome (toe twitch on ipsilateral hindpaw). Next, the current intensity was reduced in 1 μA steps until the twitch was undetectable. The lowest current at which a twitch was observed, across the most ventral electrodes, was considered resting motor threshold. That electrode was subsequently used to deliver ISMS.

Recording sessions consisted of a randomly ordered series of trials of the following general sequence: (a) ~1 min of innocuous mechanical stimulation of the receptive field; (b) 2 min of noxious mechanical stimulation of the receptive field without concurrent ISMS; (c) 2 min, 10 min, or 30 min of motor-targeted ISMS alone or 2 min, 10 min, or 30 min of motor-targeted ISMS combined with phasic noxious mechanical stimulation of the receptive field; (d) 2 min of noxious mechanical stimulation of the receptive field without concurrent ISMS; and (e) 1 min of innocuous mechanical stimulation of the receptive field without concurrent ISMS. (Note that trials of a given ISMS duration were conducted separately from trials of other ISMS durations; i.e., 10 min ISMS trials were not merely extensions of the 2 min ISMS trials, and likewise, the 30 min ISMS trials were not merely extensions of the 10 min ISMS trials.)

This trial structure enabled direct observation of the potential modulatory actions of ISMS on transmission in spinal nociceptive and non-nociceptive cutaneous pathways. By including epochs of non-nociceptive transmission as well as nociceptive transmission, it was also possible to classify neurons as nociceptive specific (NS) or wide dynamic range (WDR). Approximately 5–10 such trials were acquired per animal. Additionally, trials of spontaneous neural activity (i.e., no induced sensory transmission or ISMS) were interleaved with the sensory transmission trials. These trials averaged ~10 min each and were used both as a rate-limiting step to prevent windup of WDR neurons and to gauge overall spinal excitability and the stability of the neural recordings as the experiment progressed.

Electrical and mechanical stimulation parameters were as follows. Motor-targeted ISMS was delivered as a series of discrete, cathode-leading pulses at 7 Hz, 200 μs/phase, 0 s inter-phase interval, and 90% of resting motor threshold (range: 2–24 μA/phase), consistent with previous work demonstrating functionally meaningful enhancements of spinal motor output below a chronic SCI (1) and consistent with relative stimulation intensities frequently used in studies of ESS parameterized for ameliorating pain (i.e., 80–90% of resting motor threshold) (22, 23). Nociceptive transmission was induced by applying firm, ~1–2 sec duration pinches of the most sensitive area of the receptive field with precision forceps every ~30 sec. Non-nociceptive sensory transmission was induced by gentle touches or brushes of the dermatome with a cotton-tipped applicator.

Upon completion of electrophysiological recordings, animals were humanely euthanized and unfixed spinal cords were immediately harvested and frozen. Subsequently, spinal cords were cut into 20 μm sections and viewed under a fluorescent microscope to identify the electrode tracks (ThermoFisher Scientific; EVOS RFP light cube). Spinal cord sections were then stained with cresyl violet and/or eriochrome cyanine R to determine the location on of the electrodes relative to key morphological features of the gray matter (e.g., motor pools).

Spike train analysis and functional classification of neurons

Raw, multi-unit neural data were pre-processed off-line to remove non-physiological features (e.g., electrical noise) (The MathWorks, Inc.). Using a wavelet-based spike sorting algorithm (24), we then extracted and clustered single-unit spiking activity as described previously (20, 21) (Fig. 1b). Additional cleaning of single-unit data was achieved manually by assessing quantitative (e.g., predominance of interspike intervals < 2ms) and qualitative (e.g., non-physiological shape of the action potential or inappropriate action potential duration) criteria. Neurons that did not pass the manual verification were removed.

Sensory neurons were functionally classified as NS or WDR based on their instantaneous firing rate during the aforementioned periods of mechanical stimulation of the dermatome (20). Neurons that only responded to noxious mechanical stimulation of the dermatome were classified as NS, whereas neurons that responded both to noxious and innocuous mechanical stimuli were classified as WDR.

Statistical analyses

The primary outcome measure underpinning all statistical comparisons was instantaneous firing rate. Because the distribution of firing rates was rarely normally distributed,

descriptive statistics are presented in the text and figures as the median ± 95% confidence interval unless otherwise noted.

After functionally classifying neurons as either NS or WDR, we used Friedman's test to determine whether ISMS was associated with significant changes in the overall firing rate of each pool during periods of induced nociceptive or non-nociceptive transmission. We then stratified neurons by those that exhibited firing rate increases vs. decreases following ISMS (relative to their pre-ISMS levels) to interrogate trends within these subgroups (also utilizing Friedman's test). Missing data were rare, but stemmed from two sources: (1) cases where a neuron could not be reliably tracked during ISMS, and (2) trials in which induced nociceptive transmission failed to recruit a neuron post-ISMS. In such cases, a neuron's data was excluded from analysis.

The independent variable for these analyses was timepoint relative to ISMS, which contained levels of 'pre-ISMS', 'during-ISMS' (which could have from 1–3 discrete timepoints), and 'post-ISMS'. The dependent variable was peak instantaneous firing rate per neuron. Neurons were treated independently rather than grouped per rat, as we have previously validated (20). Post-hoc analyses compared pre-ISMS firing rates during induced nociceptive or non-nociceptive transmission to each subsequent timepoint, including post-ISMS. Dunn's test corrected for multiple comparisons.

Additional statistical tests included the following: Mann-Whitney tests to compare median percent change in firing rate across trials of different durations (e.g., median percent decrease during 2 min of ISMS vs. median percent decrease during 10 min of ISMS), and, for trials containing 30 min of ISMS, nonlinear regression to determine whether a relationship existed between the firing rate of a neuron pool (e.g., all WDR neurons) and timepoint during ISMS. All statistical analyses used a family-wise α level of 0.05.

Two additional statistical considerations should be noted. First, it cannot be assumed that each trial for a given animal included the same neurons. This is a byproduct of discriminating multi-unit extracellular recordings into single neuron spike trains, which precludes unequivocal verification and assignment of a given waveform to a specific neuron. Second, some rats did not have trials of all ISMS durations (e.g., 2 min, 10 min, 30 min). As a result, the specific population of rats/neurons in each time bin may vary slightly, leading to different absolute median firing rates (e.g., the median pre-ISMS firing rates for the 2 min trials may be slightly different than the median pre-ISMS firing rates for the 10 min trials). Therefore, we analyze and present both raw firing rates and percent change in firing rate. The validity of this dual approach relies on the assumption that the population of neurons sampled in each rat (a) is sufficiently large to provide a robust estimate of network behavior and (b) is similar across rats. The first of these factors is to some degree unknowable because it is not possible to determine the total number of NS or WDR neurons that were contained in the sampled spinal segments. This is a well-known limitation of network and systems-level neuroscience. Regarding the second factor, we found no systematic variation in firing rates across subgroups of rats or window durations for computing firing rate statistics, which supports our conclusion that the populations are comparable. This conclusion is further supported by previous work using similar techniques,

in which cluster analyses revealed no systematic differences between populations of neurons accessed from multiple rats (20).

Results

Motor-targeted ISMS immediately modulates nociceptive transmission

We recorded an average of 76 (±2) well-isolated neurons (firing rate> 0.11 Hz) per trial, including NS, WDR, and functionally unclassified neurons. We estimate that the total number of neurons recorded, across all rats, ranged from ~1,060 (i.e., 76 neurons/animal per 14 animals, under the assumption that each trial for a given rat included the same population of neurons) to ~5,800 (taking each neuron per trial per rat as independent). These neurons were distributed throughout the dorsal (~3,640) and ventral (~2,160) horns. On average, we identified 2 (±1) NS neurons and 10 (±1) WDR neurons per trial in the dorsal horn, with 1 (±1) NS neuron and 3 (±1) WDR neurons located in the superficial dorsal horn (~100–300 μm deep to the surface of the spinal cord) and the remainder in the deep dorsal horn (~400–1000 μm deep to the surface of the spinal cord). We did not convincingly identify NS or WDR neurons in the intermediate gray matter or ventral horns in these trials.

Many epidural electrical stimulation (EES) paradigms, whether parameterized to enhance movement or to suppress pain, immediately modulate neural transmission in the dorsal horn. The extent to which motor-targeted ISMS modulates neural transmission in the dorsal horn remains incompletely understood, with reports of its impact on nociceptive transmission being absent from the literature. As a first step towards understanding the impacts of ISMS on neural firing dynamics, we began by characterizing the spatial extent to which sub-motor threshold ISMS alone (i.e., *without* concurrently induced sensory transmission such as a pinch) modulates ongoing spiking.

In Fig. 2a, we show peristimulus time histograms for 46 well isolated neurons discriminated during sub-motor threshold ISMS delivered to the crural flexor motor pool (bottom and left-most electrode of the array as shown; indicated in red). We found that many of the identified neurons exhibited short-latency responses to ISMS, including neurons classified as NS or WDR (colored plots on left) as well as other, functionally unclassified neurons (in black). Longer-latency responses, indicative of highly polysynaptic interactions, were also observed. That short-latency actions were prevalent in the dorsal horn was contradictory to our expectations, given the low current intensity and relatively distant location of stimulation. The presence of both short- and long-latency dorsal horn responses strongly suggested that motor-targeted ISMS may indeed be capable of modulating sensory transmission.

We then investigated the effects of brief, 2 min epochs of ISMS on induced nociceptive transmission. Pooling across all NS neurons and, separately, all WDR neurons, we found no significant main effects of ISMS on firing rate during induced nociceptive transmission ($p = 0.81$ and $p = 0.12$, respectively). However, this seemingly null result masked robust subgroup-level modulation in both neuron pools, with a portion of neurons potentiated by ISMS and another portion depressed by ISMS. Representative examples of the depressive actions of ISMS on nociceptive transmission in two WDR neurons are shown in Fig. 2b. In total, the majority of NS neurons (60%) and 46.35% of WDR neurons exhibited lower firing

rates during induced nociceptive transmission when ISMS was ongoing than before ISMS began (Fig. 3a,b). The magnitude of change in firing rate (± 95% CI) for each category is depicted in Fig. 3c.

We next asked whether carryover effects were evident following 2 min of ISMS, despite the short duration of stimulation. We found that the overall proportion of NS and WDR neurons exhibiting depressed or potentiated firing rates during nociceptive transmission regressed towards a more even distribution (NS: 47.5% depressed vs. 52.5 potentiated; WDR: 50.27% depressed vs. 49.73 potentiated) (Fig. 3a,b). However, the *magnitude* of antinociceptive effects grew significantly in the subgroup of NS neurons depressed following ISMS, to a median percent decrease of 40.86% relative to during-ISMS levels ($p = 0.03$; Fig. 3c). The magnitude of potentiation in NS neurons remained unchanged following 2 min of ISMS ($p = 0.45$). By comparison, neither the magnitude of depression nor the magnitude of potentiation increased in WDR neurons ($p = 0.40$ for depression; $p = 0.12$ for potentiation).

Anti-nociceptive potency increases with ISMS duration

We then asked whether longer durations of ISMS would lead to additional modulation of nociceptive transmission. We began by characterizing the effects of 10 min of ISMS on neural firing dynamics. This duration parallels the timecourse over which the modulatory actions of paresthesia-based EES parameterized for pain amelioration become evident in WDR and NS neurons (25). It is also predicted to be adequate for observing sensitization or habituation in the modulated spinal networks based on the seminal studies documenting these phenomena in spinal flexion reflexes (26).

We found a significant main effect of ISMS on firing rate when pooling across all NS neurons and, separately, all WDR neurons ($p = 0.01$ and $p < 0.0001$, respectively). For NS neurons, this effect was driven by lower post-ISMS firing rates than during-ISMS firing rates across the entire pool ($p = 0.01$; pre-ISMS rate was not different than during ISMS rate, $p = 0.48$). For WDR neurons, the significant main effect was driven by lower firing rates across the entire pool both during and after ISMS relative to pre-ISMS levels (both comparisons: $p < 0.0001$). Parsing the NS and WDR neuron pools into subgroups exhibiting increased or decreased firing rates, we found that 43.08% of NS neurons and 52.82% of WDR neurons exhibited firing rate depression during 10 min of ISMS (Fig. 4a,b). The magnitude of change in firing rate (± 95% CI) for each category is depicted in Fig. 4c.

The proportions of NS and WDR neurons exhibiting firing rate depression both *increased* after ISMS was discontinued (Fig. 4a,b). Indeed, the majority of both types of neurons exhibited lower firing rates during induced nociception following 10 min of ISMS compared to pre- or during ISMS (57.58% of NS and 59.94% of WDR neurons). For NS neurons, the median percent decrease in firing rate following ISMS was significantly larger than the median percent decrease observed during ISMS ($p = 0.01$), whereas the percent increase was indistinguishable from its during-ISMS level ($p = 0.46$; Fig. 4c). WDR neurons were stratified either by a 26.68% reduction in firing rate or a 25.19% increase in firing rate post-ISMS, both of which were significantly larger than those observed during ISMS ($p < 0.0001$ for depression; $p = 0.01$ for potentiation; Fig. 4c).

Compared to 2 min of ISMS, a slightly lower proportion of NS neurons was depressed during 10 min stimulation epochs, but a greater proportion was depressed *following* 10 min stimulation epochs. Consistent with the lower proportion of NS neurons depressed during 10 min ISMS trials, their median percent increase was larger during 10 min of ISMS than that observed during 2 min of ISMS ($p = 0.03$; Fig. 5, first two columns). By comparison, the median percent decrease in firing rate during 10 min trials of ISMS was statistically indistinguishable from that observed during 2 min trials of ISMS (Fig. 5, second two columns). Neither the magnitude of firing rate increases nor the magnitude of firing rate decreases changed for NS neurons when increasing ISMS duration from 2 to 10 min (Fig. 5, columns 5–8).

In contrast to NS neurons, a greater proportion of WDR neurons was depressed during 10 min ISMS epochs than during 2 min ISMS epochs. Despite the increased number of depressed WDR neurons, the magnitude of firing rate depression was modestly lower during 10 min of ISMS than 2 min of ISMS ($p = 0.04$; Fig. 5, columns 11–12). The magnitude of firing rate increases remained unchanged during trials of 2 min and 10 min of ISMS ($p = 0.08$; Fig. 5). Following cessation of ISMS, a greater proportion of WDR neurons remained depressed following 10 min stimulation epochs compared to 2 min stimulation epochs. This was accompanied by a greater magnitude of firing rate depression in 10 min ISMS trials compared to 2 min ISMS trials, as well ($p = 0.02$; Fig. 5, last two columns).

Given that periods of spinal stimulation for pain management are longer than 10 min – often lasting from ~30 min – 2 hrs or more at a time – it was important to understand whether the overall anti-nociceptive effects observed following 10 min of ISMS would persist with increasing ISMS durations. Thus, we next investigated the effects of 30 min of ISMS on nociceptive transmission.

We found significant inverse linear relationships between firing rate and ISMS duration across the entire pool of NS neurons ($r^2 = 0.89$; $p = 0.02$; Fig. 6a) and, separately, the entire pool of WDR neurons ($r^2 = 0.94$; $p = 0.01$; Fig. 6b). To understand whether these trends were likely to reflect an overall state of reduced spinal nociceptive transmission or if they were driven by a minority of neurons in each pool with extreme changes in firing rate, we again stratified the pools by neurons that ultimately exhibited firing rate potentiation after 30 min of ISMS vs. those that exhibited firing rate depression (Figs. 7, 8). We found that the majority of all NS and WDR neurons (respectively) exhibited firing rate depression after the first 5 min of ISMS (Figs. 7a, 8a), suggesting that the effects of ISMS were indeed robust.

Three additional findings also emerged from these analyses: (1) for the subgroups of NS and WDR neurons that exhibited firing rate *increases* after ISMS, at no point during or after ISMS did the subgroup's firing rate statistically exceed its pre-ISMS firing rate (Figs. 7b, 8b); (2) for WDR neurons that exhibited firing rate *decreases* after ISMS, the subgroup's mean firing rate was significantly lower at each timepoint during and following ISMS than its pre-ISMS level ($p = 0.01$, $p < 0.01$, $p < 0.0001$, and $p < 0.0001$, respectively; Fig. 8b); and (3) the magnitude of the largest percent increase in firing rate for each subgroup was not significantly different than the magnitude of the percent decrease at the same timepoint (Figs. 7c, 8c).

However, it should be noted that we did observe two instances across the 2 min and 10 min ISMS trials where the percent increase in firing rate was greater than the corresponding percent decrease. These cases were WDR neurons during 2 min ISMS (28.74% vs. 20.34%, $p = 0.02$; Fig. 3c) and NS neurons during 10 min of ISMS (56.41% vs. 24.89%, $p < 0.01$; Fig. 4c). These observations raised the question of whether ISMS could have induced a transient state of increased nociceptive transmission that habituated with longer durations of stimulation (e.g., ≥30 min). To address this issue, we determined whether the pre-ISMS firing rates (during induced nociceptive transmission) of neurons that were ultimately depressed by ISMS differed from the during-ISMS firing rates of neurons that were potentiated by ISMS (also during induced nociceptive transmission). In both cases, we found no significant differences (for WDR neurons and 2 min ISMS, $p = 0.28$; for NS neurons and 10 min ISMS, $p = 0.13$).

As an example, take NS neurons that increased their firing rate during 10 min of ISMS. This subgroup exhibited the most extreme percent increase of all groups, 56.41%. However, its median discharge rate when nociceptive transmission was induced during ISMS, 21.65 (13.11–32.52) Hz, was statistically indistinguishable from the pre-ISMS firing rate (14.49 Hz) of NS neurons that were ultimately *depressed* by ISMS. That is, while some NS neurons were indeed potentiated by ISMS, the level of potentiation merely brought them to the baseline level of the remainder of the population. This finding was mirrored by WDR neurons that increased their firing rate during and after 2 min of ISMS.

Considering that most NS and WDR neurons were depressed by 10 and 30 min of ISMS, and that the overall pools of NS and WDR neurons exhibited progressive firing rate reductions with increasing ISMS duration, these findings support the conclusion that the observed firing rate increases were unlikely to have caused a net increase in nociceptive transmission. Rather, the opposite conclusion appears more plausible: ISMS reduced overall nociceptive transmission.

Motor-targeted ISMS does not potentiate non-nociceptive cutaneous transmission

Spinal stimulation paradigms parameterized to enhance motor output post-SCI, whether ESS or ISMS, are generally hypothesized to act in part by engaging non-nociceptive sensory afferent pathways that provide excitatory synaptic drive to motoneuron pools (1, 14, 27). Many ESS paradigms for pain relief presumably modulate an overlapping set of pathways (14, 15, 19), which have direct and indirect connections with WDR neurons. However, for ISMS, it is not known whether those modulatory actions augment WDR firing rates during periods of induced non-nociceptive transmission. Thus, we characterized WDR firing rates while lightly touching/brushing the plantar surface of the hindpaw (i.e., the same paw/dermatome used to characterize nociceptive transmission). We found a significant *decrease* in WDR firing rates during non-nociceptive sensory transmission within the first 2 min of ISMS ($p<0.0001$, Fig. 9, left). This effect habituated over the course of 10 min of ISMS, with WDR firing rates recovering to but not exceeding their pre-ISMS baseline levels (Fig. 9, right).

Discussion

Our primary finding is that motor-targeted ISMS immediately and persistently modulates concurrent nociceptive transmission, decreasing the prevalence and magnitude of spinal responses to noxious peripheral stimuli. These results highlight a potential new approach for managing the debilitating sensorimotor consequences of SCI and suggest that it may be possible to use ISMS to develop additional therapies specifically intended to provide multi-modal rehabilitation.

Motor-targeted ISMS results in depression of spinal responses to painful peripheral stimuli

To some extent, off-target effects of ISMS on sensory transmission were expected, even at sub-motor threshold intensities. Indeed, ISMS delivered to spinal motor pools activates sensory afferents, premotor and other intercalated interneurons, and ascending/descending fibers of passage at lower electrical current intensities than motoneuron cell bodies or motor axons (27, 28). As a result, the spatiotemporal profile of neuromodulation that results from ISMS far exceeds that which would be expected from direct current spread alone. However, it was not clear *a priori* whether ISMS would modulate high-threshold nociceptive transmission at all, let alone drive robust potentiation or depression of neurons in these networks. Yet, we found that the anti-nociceptive effects of motor-targeted ISMS began almost immediately (<2 min), with the majority of all identified NS and WDR neurons exhibiting depressed responses to induced nociceptive transmission within the first 10 min of stimulation. And while the average proportion of NS neurons (67%) and WDR neurons (68%) exhibiting depressed nociceptive responses remained effectively constant for the duration of ISMS (Figs. 7, 8), the magnitude of depression increased over this span (Figs. 6–8).

At a more granular level, two additional observations bear reiterating. First, the proportion of neurons exhibiting depressed responses to induced nociceptive transmission and the magnitude of depression per neuron both appeared to increase after ISMS was discontinued. It is not clear whether these effects are unique to ISMS, as similar effects may occur with ESS but remain masked by electrical stimulation artifacts. Another particularly intriguing finding was that motor-targeted ISMS caused an immediate decrease in WDR responses to non-nociceptive transmission that habituated over 10 minutes of stimulation. This effect was contrary to our prediction because ISMS delivered to motor pools has been reported to antidromically activate Aβ afferents (27), which provide excitatory synaptic drive to WDR neurons. This observation also revealed an unexpected degree of modal specificity in the modulatory actions of ISMS, given that decreased nociceptive responses in the same neurons did not habituate over 10 min of ISMS.

Diverse mechanisms may underlie the anti-nociceptive effects of ISMS

Below, we describe possible mechanisms contributing to our observations. However, it should first be reiterated that ISMS almost assuredly resulted in an unnatural spatiotemporal mixture of synaptic inputs to NS and WDR neurons. This is both because we delivered ISMS to spinal motor pools in the ventral horn, effectively bypassing orthodromic activation of terminal branches of axons presynaptically coupled to NS and WDR neurons in the dorsal

horn, and because we delivered ISMS at sub-motor threshold electrical current intensities, which likely precluded direct activation of many NS, WDR, and interneuron cell bodies in the dorsal horn.

The near immediate anti-nociceptive effects of motor-targeted ISMS and the relatively constant proportion of neurons exhibiting depressed firing rates during stimulation presumably reflects the presence of active inhibition. A role for disfacilitation cannot be excluded, although it would seem to be less likely given the continued injection of current via ISMS. Under the nominal assumption that the interneurons and axons modulated by ISMS act on WDR and NS neurons in accordance with the gate control theory, reduced firing rates via active inhibition would be expected. And indeed, there is some empirical evidence that paresthesia-based EES for neuropathic pain acts in at least partial accordance with this mechanism (29). But the view that EES acts exclusively through this mechanism is overly reductionist (15, 22, 23), and moreover, ISMS and EES presumably modulate different, if somewhat overlapping, mixtures of spinal neurons and axons.

That we observed progressive increases in the magnitude of firing rate depression with increasing ISMS duration (Fig. 6) could suggest that ISMS promoted induction of long-term depression (LTD) in the modulated neurons. Induction of LTD could also explain why the anti-nociceptive effects of ISMS persisted beyond the duration of stimulation. And together, these observations further support the notion that a gating-like mechanism is insufficient to fully explain the actions of ISMS: as classically understood, such a mechanism would require ongoing convergence of nociceptive and non-nociceptive cutaneous transmission (the latter of which was mediated via ISMS) and would be predicted to result in a relatively constant magnitude of firing rate depression.

What could underlie the observation of increased nociceptive depression post-ISMS? One possibility is that it is paradoxically related to the facilitatory effects of ISMS. At the level of the neuron pool, ISMS was associated with increased firing rates in a subset of NS and WDR neurons. Presumably, the facilitatory actions of ISMS were sufficient in those neurons to potentiate their responses to nociceptive transmission, whether through direct excitation, disinhibition, or both. This potentiation could have occurred through relatively specific and repeatable (albeit unknown) pathways or through variable combinations of synaptic inputs possibly via a stochastic resonance-like effect (30, 31). Regardless, it is reasonable to think that when ISMS was discontinued, sensory afferent transmission alone was either insufficient to drive spiking in that subset of NS and WDR neurons or that it was only sufficient to drive them at a lower firing rate. However, this explanation relies on the assumption that the subset of NS and WDR neurons facilitated by ISMS had preferentially higher firing rates during nociceptive transmission than the remainder of their respective pools, and such an observation was not borne out by the experimental data.

Looking instead at the level of an individual neuron, the observation of increased nociceptive depression post-ISMS could reflect synaptic modification consistent with the dual-process theory of plasticity (32, 33). ISMS delivered at a given electrical current intensity will indiscriminately modulate cell bodies and axons within a range of input resistances/conductances and distances from the stimulating electrode. Consequently, ISMS would have

presumably coactivated excitatory, inhibitory, and endogenous neuromodulatory inputs to NS and WDR neurons during stimulation. These inputs would have effectively competed across spatiotemporal scales to drive net depression, habituation, or facilitation of the post-synaptic neurons. If sufficiently reinforced (by ongoing ISMS), these depressive or facilitatory actions could have led to enduring modifications of synaptic function via long-term depression or potentiation.

ISMS-driven facilitation would be expected to counter the potency of concurrent ISMS-driven inhibition, tempering the magnitude of firing rate depression observed during ISMS. Yet, if the net effect of ISMS was still to depress a neuron's response to nociceptive transmission leading to LTD, then we would predict that the firing rate of that neuron would be lower after ISMS than its rate during ISMS due to the absence of concurrent stimulation-induced facilitation. Our results support this general mechanism. However, our results cannot identify the precise mixture of synapses or transmitter networks that led to the changes in synaptic efficacy or whether these changes are homosynaptic, heterosynaptic, or both.

Another potential mechanism that could have contributed to our observations is ISMS-promoted release of endogenous neuromodulators from terminal branches of bulbospinal axons. The monoamines serotonin and norepinephrine are one example. Monoaminergic axons and receptors are interposed throughout sensory and motor-dominant regions of the spinal gray matter, where they directly and indirectly modify the input-output function NS neurons, WDR neurons, and motoneurons (34–38). Interestingly, serotonin and norepinephrine differentially impact the overall excitability of spinal motor and nociceptive networks. They are potently excitatory to motoneurons, amplifying their responses to excitatory synaptic inputs by 5x or more by activating persistent inward currents in motoneuron dendrites (39, 40). In contrast, they are generally inhibitory in nociceptive networks (particularly norepinephrine) (36, 37, 41). Given these opposing effects, a contribution from monoamines would be phenomenologically consistent with many of our observations (i.e., decreased spinal responses to nociceptive transmission with concomitant increases in spinal motor output). And indeed, there is evidence that a portion of the antinociceptive effects of EES are mediated by enhanced serotonergic signaling (23).

However, the extent to which motor-targeted ISMS can engage monoaminergic axons innervating the dorsal horn is unclear. Indeed, monoaminergic fibers that terminate in the ventral horn are anatomically discrete from those terminating in the dorsal horn. For example, projections from the raphe pallidus and obscurus descend in the lateral and ventral funiculi before terminating in the ventral horn and intermediate zone, whereas projections from the raphe magnus descend in the dorsolateral funiculus before terminating in the dorsal horn (35, 37, 42). Thus, a single point-source of sub-motor threshold current in the ventral horn is not optimally juxtaposed to modulate the dorsally projecting fibers. Nevertheless, the surprisingly wide spatial extent of ISMS-driven neuromodulation suggests that it may have been possible to recruit both tracts simultaneously.

Finally, we return to the response habituation of WDR neurons during non-nociceptive sensory transmission. As aforementioned, response habituation was not observed in the

same neurons during nociceptive transmission. We do not expect that this differential response was a direct effect of ISMS, because the ISMS parameters remained constant between periods of nociceptive and non-nociceptive transmission. Rather, we speculate that it was due to afferent-driven engagement of different interneuron networks during nociceptive vs. non-nociceptive transmission leading to a different evolution of the dual-process theory. However, we cannot rule out the possibility that ISMS-induced antidromic spikes collided with afferent-driven orthodromic spikes and reduced the net firing rate of a given neuron or that ISMS-induced antidromic spiking itself differentially modulated plasticity across synapses mediating nociceptive vs. non-nociceptive transmission onto WDRs.

Translational potential: depression of spinal responses to painful peripheral stimuli

Absent direct behavioral evidence, it is difficult to connect the observed anti-nociceptive effects of ISMS with the behavioral experience of pain. Further complicating behavioral contextualization of our findings is lack of knowledge of what proportion of the sampled NS and WDR neurons were output neurons of the spinothalamic tract vs. what proportion remained in segmental networks. However, given that the majority of NS and WDR neurons exhibited depressed responses to nociceptive transmission during and following ISMS and the fact that we accessed these neurons in spinal regions known to contain output neurons, we speculate that transmission in the spinothalamic tract was reduced to some extent.

It should also be reiterated that this study was not an efficacy trial of ISMS for management of neuropathic pain. Rather, it was intended to explore the potential effects of motor-targeted ISMS on nociceptive transmission. As such, the specific stimulation parameters utilized here are not likely to be optimally efficacious for pain management. It is also not clear if these multimodal effects are unique to ISMS or if they would generalize to EES; future work in this area is clearly warranted. Nevertheless, several of our observations suggest that ISMS holds translational potential for neuropathic pain applications.

First, the timecourse over which the majority of anti-nociceptive effects were realized and the magnitude of firing rate depression both tracked closely with EES paradigms intended specifically to treat pain (25, 29). For example, across a range of paresthesia-based and paresthesia-free EES parameterizations, ~40–80% of NS and WDR neurons exhibited depressed responses to induced nociceptive transmission following 5 min of stimulation (25). Our findings are consistent with these results. Likewise, for the neurons that were depressed by ISMS, the magnitude of depression appears to be at least as great (on average) as that reported with EES (25). One difference between our observations with ISMS and the EES literature is that ISMS robustly decreased nociceptive transmission in neurologically intact rats, whereas EES appears to be effective primarily when a state of dorsal horn hyperexcitability or chronic neuropathic pain is preexisting (43, 44).

Second, we found no evidence of response habituation in the anti-nociceptive effects of ISMS during or following 30 min of stimulation. On the contrary, the magnitude of depression increased monotonically over this span for both the NS and WDR populations. The extent to which this trend would continue over longer durations (days, weeks, etc.) is unknown. But the initial finding is encouraging considering that nocifensive flexion

reflex responses habituate on much shorter timescales during innocuous peripheral nerve stimulation (26).

Third, we found that the anti-nociceptive effects of ISMS persisted after stimulation was discontinued. Although this study only investigated relatively short periods of ISMS and was not intended to systematically characterize their washout timecourse, previous work indicates that functionally relevant changes in spinal motor output can be observed weeks after discontinuation of ISMS when delivered as part of a targeted rehabilitation program (1). Realization of similarly enduring therapeutic benefits for pain amelioration would be of considerable translational significance, as a central challenge in the neuromodulation field continues to be development of paradigms whose therapeutic benefits meaningfully outlast the duration of stimulation.

And lastly, together with the previously documented ability of ISMS to enhance spinal motor output (1, 5, 45–47), our findings suggest that ISMS may be particularly well suited for individuals living with SCI. Indeed, depression of NS and WDR neurons would be predicted to reduce hyperalgesia and allodynia, two of the most common manifestations of below-level SCI-NP (8). And by not enhancing WDR responses to non-nociceptive cutaneous transmission, ISMS-based therapies may avoid exacerbating the debilitating spasms and spasticity experienced by many individuals living with SCI.

Translational potential: practical considerations

Our use of ISMS was motivated by the following factors. First, ISMS confers an added degree of specificity over EES because ISMS enables delivery of electrical current directly to spinal motor pools. Second, use of ISMS allowed us to reconcile differences in electrical current intensities used in EES paradigms parameterized to enhance motor output vs. those parameterized to ameliorate neuropathic pain. Specifically, motor-targeted EES is typically delivered at suprathreshold intensity for evoking muscle contractions (2–4), whereas EES for pain is delivered at sub-motor threshold intensities (22, 23); preclinical evidence has demonstrated that ISMS can meaningfully enhance voluntary motor output below an SCI even when delivered at sub-motor threshold intensities (1). And lastly, we and others have demonstrated the potential therapeutic value of ISMS for a range of SCI-related impairments including motor rehabilitation (1, 5, 45–47), urinary function (48–50), and respiration (51, 52), and we have shown that it is particularly effective at driving enduring, functionally relevant neural plasticity following SCI (1).

Several lines of scientific and technical research will be required to advance ISMS-based approaches for neuropathic pain (nominally) and/or sensorimotor impairments (more broadly) along a path towards potential clinical realization. Many of these lines can evolve in parallel. For example, ISMS parameter optimization studies (53), including computational modeling, comparative neuroanatomical studies (54), and longitudinal electrophysiological studies in animal models, can occur alongside biocompatibility studies (55–57). Likewise, pre-clinical efficacy studies can be conducted in parallel with mechanical design work on the implants themselves.

The following specific areas of research will be essential for successful translation of ISMS-based therapies to the clinic. First, it will be necessary to determine the optimal location(s) in the gray matter to deliver ISMS both for pain-specific applications and for sensorimotor/multi-modal applications. Particularly for heterogeneous conditions like SCI, optimization may require tailoring the implant location and stimulation parameters to the individual patient. The potential utility of patient-level modeling has recently been demonstrated for EES (58). Second, a deeper understanding of the neural mechanisms underlying ISMS-driven effects on nociceptive transmission is required. Findings in this area are expected both to facilitate selection of stimulation parameters and to reveal possible opportunities for enhancing the efficacy of ISMS through the addition of adjuvants (e.g., ISMS combined with targeted neuropharmacology).

Another open question for translational applications of ISMS is determining to what extent ISMS directly blocks axonal transmission, whether in segmental or ascending fibers. Indeed, an emerging body of work is focusing on whether the reportedly increased pain relief and comparatively few paresthesias associated with kilohertz frequency EES are related to this mechanism (59–62). And finally, from a mechanical design standpoint, a pressing area of research will continue to be determining how and where to secure the ISMS implant such that the microwires and stimulator package do not damage the spinal cord, particularly as it glides in the spinal canal. Work in this area is ongoing (63–66).

Given the translational work remaining to determine if ISMS will be a viable clinical alternative to EES, it is also instructive to consider the potential for EES to be used in a multi-modal rehabilitation context. Indeed, EES will likely continue to serve as the only implantable neuromodulatory option in the interim. Although EES has traditionally been parameterized in a domain-specific manner (e.g., for chronic pain *or* locomotor rehabilitation, not both), there is reason to posit that it may also be capable of providing multi-modal therapeutic benefits. Most simply, this potential is evinced by the well documented ability of EES to (separately) alleviate pain as well as to enhance voluntary motor output. Beneficial off-target effects of EES have also been anecdotally reported (e.g., on autonomic functions), but neither the incidence of such effects nor their clinical significance has been systematically investigated.

The putative mechanism(s) of action of EES, as well as its ability to modify both nociplastic and neuropathic pain syndromes, also point towards an ability to simultaneously modulate sensory and motor-related neural transmission. However, from a clinical standpoint it is less clear whether such multi-modal effects could realistically be achieved. For example, traditional EES parameterized for pain amelioration utilizes stimulation intensities subthreshold for enhancing voluntary motor output. Nevertheless, assessing the ability of EES to simultaneously modulate sensory and motor function would be straightforward, as persons living with myriad such deficits are already implanted with EES systems and many relevant outcome measures could be efficiently captured by validated clinical scales during clinic or lab visits. Ultimately, EES and ISMS may have unique clinical benefits and be indicated in different circumstances. But without a robust picture of their intended and off-target effects, these benefits may prove difficult to ascertain. The neuromodulation

and rehabilitation fields would benefit greatly from routine collection and dissemination of EES-associated multi-modal outcome measures.

Conclusions

These results demonstrate that ISMS parameterized to enhance motor output immediately and persistently modulates transmission in spinal nociceptive pathways, resulting in an overall net decrease in nociceptive transmission. While a more granular understanding of the underlying mechanisms will enable simultaneous optimization of ISMS for motor rehabilitation and SCI-NP, these results highlight the potential for spinal stimulation paradigms to deliver true multi-modal therapeutic benefits.

Acknowledgements:

This work was supported by National Institutes of Health grants K12HD073945 and 7R01NS111234, both to JGM.

Abbreviations:

EES	epidural electrical stimulation
ISMS	intraspinal microstimulation
NS	nociceptive specific neuron
SCI	spinal cord injury
SCI-NP	spinal cord injury-related neuropathic pain
WDR	wide dynamic range neuron

References

1. McPherson JG, Miller RR, Perlmutter SI. Targeted, activity-dependent spinal stimulation produces long-lasting motor recovery in chronic cervical spinal cord injury. Proc Natl Acad Sci U S A. 2015;112(39):12193–8. [PubMed: 26371306]
2. Wagner FB, Mignardot JB, Le Goff-Mignardot CG, Demesmaeker R, Komi S, Capogrosso M, et al. Targeted neurotechnology restores walking in humans with spinal cord injury. Nature. 2018;563(7729):65–71. [PubMed: 30382197]
3. Angeli CA, Boakye M, Morton RA, Vogt J, Benton K, Chen Y, et al. Recovery of Over-Ground Walking after Chronic Motor Complete Spinal Cord Injury. N Engl J Med. 2018;379(13):1244–50. [PubMed: 30247091]
4. Rowald A, Komi S, Demesmaeker R, Baaklini E, Hernandez-Charpak SD, Paoles E, et al. Activity-dependent spinal cord neuromodulation rapidly restores trunk and leg motor functions after complete paralysis. Nat Med. 2022;28(2):260–71. [PubMed: 35132264]
5. Holinski BJ, Mazurek KA, Everaert DG, Toossi A, Lucas-Osma AM, Troyk P, et al. Intraspinal microstimulation produces over-ground walking in anesthetized cats. J Neural Eng. 2016;13(5):056016. [PubMed: 27619069]
6. Dimitrijevic MR, Gerasimenko Y, Pinter MM. Evidence for a spinal central pattern generator in humans. Ann N Y Acad Sci. 1998;860:360–76. [PubMed: 9928325]
7. Harkema S, Gerasimenko Y, Hodes J, Burdick J, Angeli C, Chen Y, et al. Effect of epidural stimulation of the lumbosacral spinal cord on voluntary movement, standing, and assisted stepping after motor complete paraplegia: a case study. Lancet. 2011;377(9781):1938–47. [PubMed: 21601270]

8. National Spinal Cord Injury Statistics CenterAnnual Report [Internet]. University of Alabama. 2020.
9. Dworkin RH, O'Connor AB, Kent J, Mackey SC, Raja SN, Stacey BR, et al. Interventional management of neuropathic pain: NeuPSIG recommendations. Pain. 2013;154(11):2249–61. [PubMed: 23748119]
10. Thomson S, Huygen F, Prangnell S, Baranidharan G, Belaid H, Billet B, et al. Applicability and Validity of an e-Health Tool for the Appropriate Referral and Selection of Patients With Chronic Pain for Spinal Cord Stimulation: Results From a European Retrospective Study. Neuromodulation. 2022.
11. Karri J, Joshi M, Polson G, Tang T, Lee M, Orhurhu V, et al. Spinal Cord Stimulation for Chronic Pain Syndromes: A Review of Considerations in Practice Management. Pain Physician. 2020;23(6):599–616. [PubMed: 33185378]
12. Cruccu G, Garcia-Larrea L, Hansson P, Keindl M, Lefaucheur JP, Paulus W, et al. EAN guidelines on central neurostimulation therapy in chronic pain conditions. Eur J Neurol. 2016;23(10):1489–99. [PubMed: 27511815]
13. Duan W, Huang Q, Yang F, He SQ, Guan Y. Spinal Cord Stimulation Attenuates Below-Level Mechanical Hypersensitivity in Rats After Thoracic Spinal Cord Injury. Neuromodulation. 2021;24(1):33–42. [PubMed: 32770848]
14. Formento E, Minassian K, Wagner F, Mignardot JB, Le Goff-Mignardot CG, Rowald A, et al. Electrical spinal cord stimulation must preserve proprioception to enable locomotion in humans with spinal cord injury. Nat Neurosci. 2018;21(12):1728–41. [PubMed: 30382196]
15. Linderoth B, Foreman RD. Conventional and Novel Spinal Stimulation Algorithms: Hypothetical Mechanisms of Action and Comments on Outcomes. Neuromodulation. 2017;20(6):525–33. [PubMed: 28568898]
16. Moraud EM, Capogrosso M, Formento E, Wenger N, DiGiovanna J, Courtine G, et al. Mechanisms Underlying the Neuromodulation of Spinal Circuits for Correcting Gait and Balance Deficits after Spinal Cord Injury. Neuron. 2016;89(4):814–28. [PubMed: 26853304]
17. Wenger N, Moraud EM, Gandar J, Musienko P, Capogrosso M, Baud L, et al. Spatiotemporal neuromodulation therapies engaging muscle synergies improve motor control after spinal cord injury. Nat Med. 2016;22(2):138–45. [PubMed: 26779815]
18. Ibanez J, Angeli CA, Harkema SJ, Farina D, Rejc E. Recruitment order of motor neurons promoted by epidural stimulation in individuals with spinal cord injury. J Appl Physiol (1985). 2021;131(3):1100–10. [PubMed: 34382840]
19. Yang F, Xu Q, Cheong YK, Shechter R, Sdrulla A, He SQ, et al. Comparison of intensity-dependent inhibition of spinal wide-dynamic range neurons by dorsal column and peripheral nerve stimulation in a rat model of neuropathic pain. Eur J Pain. 2014;18(7):978–88. [PubMed: 24390782]
20. Bandres MF, Gomes J, McPherson JG. Spontaneous Multimodal Neural Transmission Suggests That Adult Spinal Networks Maintain an Intrinsic State of Readiness to Execute Sensorimotor Behaviors. J Neurosci. 2021;41(38):7978–90. [PubMed: 34380765]
21. McPherson JG, Bandres MF. Spontaneous neural synchrony links intrinsic spinal sensory and motor networks during unconsciousness. Elife. 2021;10.
22. Meyerson BA, Linderoth B. Mode of action of spinal cord stimulation in neuropathic pain. J Pain Symptom Manage. 2006;31(4 Suppl):S6–12. [PubMed: 16647596]
23. Song Z, Ultenius C, Meyerson BA, Linderoth B. Pain relief by spinal cord stimulation involves serotonergic mechanisms: an experimental study in a rat model of mononeuropathy. Pain. 2009;147(1–3):241–8. [PubMed: 19836134]
24. Quiroga RQ, Nadasdy Z, Ben-Shaul Y. Unsupervised spike detection and sorting with wavelets and superparamagnetic clustering. Neural Comput. 2004;16(8):1661–87. [PubMed: 15228749]
25. Li S, Farber JP, Linderoth B, Chen J, Foreman RD. Spinal Cord Stimulation With "Conventional Clinical" and Higher Frequencies on Activity and Responses of Spinal Neurons to Noxious Stimuli: An Animal Study. Neuromodulation. 2018;21(5):440–7. [PubMed: 29164752]
26. Groves PM, De Marco R, Thompson RF. Habituation and sensitization of spinal interneuron activity in acute spinal cat. Brain Res. 1969;14(2):521–5. [PubMed: 5794923]

27. Gaunt RA, Prochazka A, Mushahwar VK, Guevremont L, Ellaway PH. Intraspinal microstimulation excites multisegmental sensory afferents at lower stimulus levels than local alpha-motoneuron responses. J Neurophysiol. 2006;96(6):2995–3005. [PubMed: 16943320]
28. Gustafsson B, Jankowska E. Direct and indirect activation of nerve cells by electrical pulses applied extracellularly. J Physiol. 1976;258(1):33–61. [PubMed: 940071]
29. Guan Y, Wacnik PW, Yang F, Carteret AF, Chung CY, Meyer RA, et al. Spinal cord stimulation-induced analgesia: electrical stimulation of dorsal column and dorsal roots attenuates dorsal horn neuronal excitability in neuropathic rats. Anesthesiology. 2010;113(6):1392–405. [PubMed: 21068658]
30. Faisal AA, Selen LP, Wolpert DM. Noise in the nervous system. Nat Rev Neurosci. 2008;9(4):292–303. [PubMed: 18319728]
31. Stein RB, Gossen ER, Jones KE. Neuronal variability: noise or part of the signal? Nat Rev Neurosci. 2005;6(5):389–97. [PubMed: 15861181]
32. Groves PM, Thompson RF. Habituation: a dual-process theory. Psychol Rev. 1970;77(5):419–50. [PubMed: 4319167]
33. Prescott SA. Interactions between depression and facilitation within neural networks: updating the dual-process theory of plasticity. Learn Mem. 1998;5(6):446–66. [PubMed: 10489261]
34. Westlund KN, Bowker RM, Ziegler MG, Coulter JD. Noradrenergic projections to the spinal cord of the rat. Brain Res. 1983;263(1):15–31. [PubMed: 6839168]
35. Holstege JC, Kuypers HG. Brainstem projections to spinal motoneurons: an update. Neuroscience. 1987;23(3):809–21. [PubMed: 2893995]
36. Jones SL. Descending noradrenergic influences on pain. Prog Brain Res. 1991;88:381–94. [PubMed: 1813927]
37. Millan MJ. Descending control of pain. Prog Neurobiol. 2002;66(6):355–474. [PubMed: 12034378]
38. Ruda MA. Spinal dorsal horn circuitry involved in the brain stem control of nociception. Prog Brain Res. 1988;77:129–40. [PubMed: 3064164]
39. Heckman CJ, Lee RH, Brownstone RM. Hyperexcitable dendrites in motoneurons and their neuromodulatory control during motor behavior. Trends Neurosci. 2003;26(12):688–95. [PubMed: 14624854]
40. Powers RK, Elbasiouny SM, Rymer WZ, Heckman CJ. Contribution of intrinsic properties and synaptic inputs to motoneuron discharge patterns: a simulation study. J Neurophysiol. 2012;107(3):808–23. [PubMed: 22031773]
41. Kucharczyk MW, Di Domenico F, Bannister K. Distinct brainstem to spinal cord noradrenergic pathways inversely regulate spinal neuronal activity. Brain. 2022.
42. Willis WD Jr. Anatomy and physiology of descending control of nociceptive responses of dorsal horn neurons: comprehensive review. Prog Brain Res. 1988;77:1–29.
43. Yakhnitsa V, Linderoth B, Meyerson BA. Spinal cord stimulation attenuates dorsal horn neuronal hyperexcitability in a rat model of mononeuropathy. Pain. 1999;79(2–3):223–33. [PubMed: 10068168]
44. Yang F, Zhang C, Xu Q, Tiwari V, He SQ, Wang Y, et al. Electrical stimulation of dorsal root entry zone attenuates wide-dynamic-range neuronal activity in rats. Neuromodulation. 2015;18(1):33–40; discussion [PubMed: 25308522]
45. Bamford JA, Mushahwar VK. Intraspinal microstimulation for the recovery of function following spinal cord injury. Prog Brain Res. 2011;194:227–39. [PubMed: 21867807]
46. Kasten MR, Sunshine MD, Secrist ES, Horner PJ, Moritz CT. Therapeutic intraspinal microstimulation improves forelimb function after cervical contusion injury. J Neural Eng. 2013;10(4):044001. [PubMed: 23715242]
47. Sunshine MD, Cho FS, Lockwood DR, Fechko AS, Kasten MR, Moritz CT. Cervical intraspinal microstimulation evokes robust forelimb movements before and after injury. J Neural Eng. 2013;10(3):036001. [PubMed: 23548462]
48. Grill WM, Bhadra N, Wang B. Bladder and urethral pressures evoked by microstimulation of the sacral spinal cord in cats. Brain Res. 1999;836(1–2):19–30. [PubMed: 10415401]

49. Pikov V, Bullara L, McCreery DB. Intraspinal stimulation for bladder voiding in cats before and after chronic spinal cord injury. J Neural Eng. 2007;4(4):356–68. [PubMed: 18057503]
50. Pikov V, McCreery DB, Han M. Intraspinal stimulation with a silicon-based 3D chronic microelectrode array for bladder voiding in cats. J Neural Eng. 2020;17(6).
51. Mercier LM, Gonzalez-Rothi EJ, Streeter KA, Posgai SS, Poirier AS, Fuller DD, et al. Intraspinal microstimulation and diaphragm activation after cervical spinal cord injury. J Neurophysiol. 2017;117(2):767–76. [PubMed: 27881723]
52. Sunshine MD, Ganji CN, Reier PJ, Fuller DD, Moritz CT. Intraspinal microstimulation for respiratory muscle activation. Exp Neurol. 2018;302:93–103. [PubMed: 29305050]
53. Roshani A, Erfanian A. The Effects of Stimulation Strategy on Joint Movement Elicited by Intraspinal Microstimulation. IEEE Trans Neural Syst Rehabil Eng. 2016;24(7):794–805. [PubMed: 26685256]
54. Toossi A, Bergin B, Marefatallah M, Parhizi B, Tyreman N, Everaert DG, et al. Comparative neuroanatomy of the lumbosacral spinal cord of the rat, cat, pig, monkey, and human. Sci Rep. 2021;11(1):1955. [PubMed: 33479371]
55. Roszko DA, Mirkiani S, Tyreman N, Wilson D, Toossi A, Mushahwar VK. Laser-microfabricated polymer multielectrodes for intraspinal microstimulation. IEEE Trans Biomed Eng. 2022;PP.
56. Vara H, Collazos-Castro JE. Enhanced spinal cord microstimulation using conducting polymer-coated carbon microfibers. Acta Biomater. 2019;90:71–86. [PubMed: 30904548]
57. Bamford JA, Todd KG, Mushahwar VK. The effects of intraspinal microstimulation on spinal cord tissue in the rat. Biomaterials. 2010;31(21):5552–63. [PubMed: 20430436]
58. Lempka SF, Zander HJ, Anaya CJ, Wyant A, Ozinga JGt, Machado AG. Patient-Specific Analysis of Neural Activation During Spinal Cord Stimulation for Pain. Neuromodulation. 2020;23(5):572–81. [PubMed: 31464040]
59. Lempka SF, McIntyre CC, Kilgore KL, Machado AG. Computational analysis of kilohertz frequency spinal cord stimulation for chronic pain management. Anesthesiology. 2015;122(6):1362–76. [PubMed: 25822589]
60. Crosby ND, Janik JJ, Grill WM. Modulation of activity and conduction in single dorsal column axons by kilohertz-frequency spinal cord stimulation. J Neurophysiol. 2017;117(1):136–47. [PubMed: 27760823]
61. Arle JE, Mei L, Carlson KW, Shils JL. High-Frequency Stimulation of Dorsal Column Axons: Potential Underlying Mechanism of Paresthesia-Free Neuropathic Pain Relief. Neuromodulation. 2016;19(4):385–97. [PubMed: 27145196]
62. Rogers ER, Zander HJ, Lempka SF. Neural Recruitment During Conventional, Burst, and 10-kHz Spinal Cord Stimulation for Pain. J Pain. 2022;23(3):434–49. [PubMed: 34583022]
63. Toossi A, Everaert DG, Seres P, Jaremko JL, Robinson K, Kao CC, et al. Ultrasound-guided spinal stereotactic system for intraspinal implants. J Neurosurg Spine. 2018;29(3):292–305. [PubMed: 29905525]
64. Bamford JA, Marc Lebel R, Parseyan K, Mushahwar VK. The Fabrication, Implantation, and Stability of Intraspinal Microwire Arrays in the Spinal Cord of Cat and Rat. IEEE Trans Neural Syst Rehabil Eng. 2017;25(3):287–96. [PubMed: 28113558]
65. Khaled I, Elmallah S, Cheng C, Moussa WA, Mushahwar VK, Elias AL. A flexible base electrode array for intraspinal microstimulation. IEEE Trans Biomed Eng. 2013;60(10):2904–13. [PubMed: 23744656]
66. Tawakol O, Mushahwar VK, Troyk PR. The use of digital image correlation for measurement of strain fields in a novel wireless intraspinal microstimulation interface. Artif Organs. 2022.

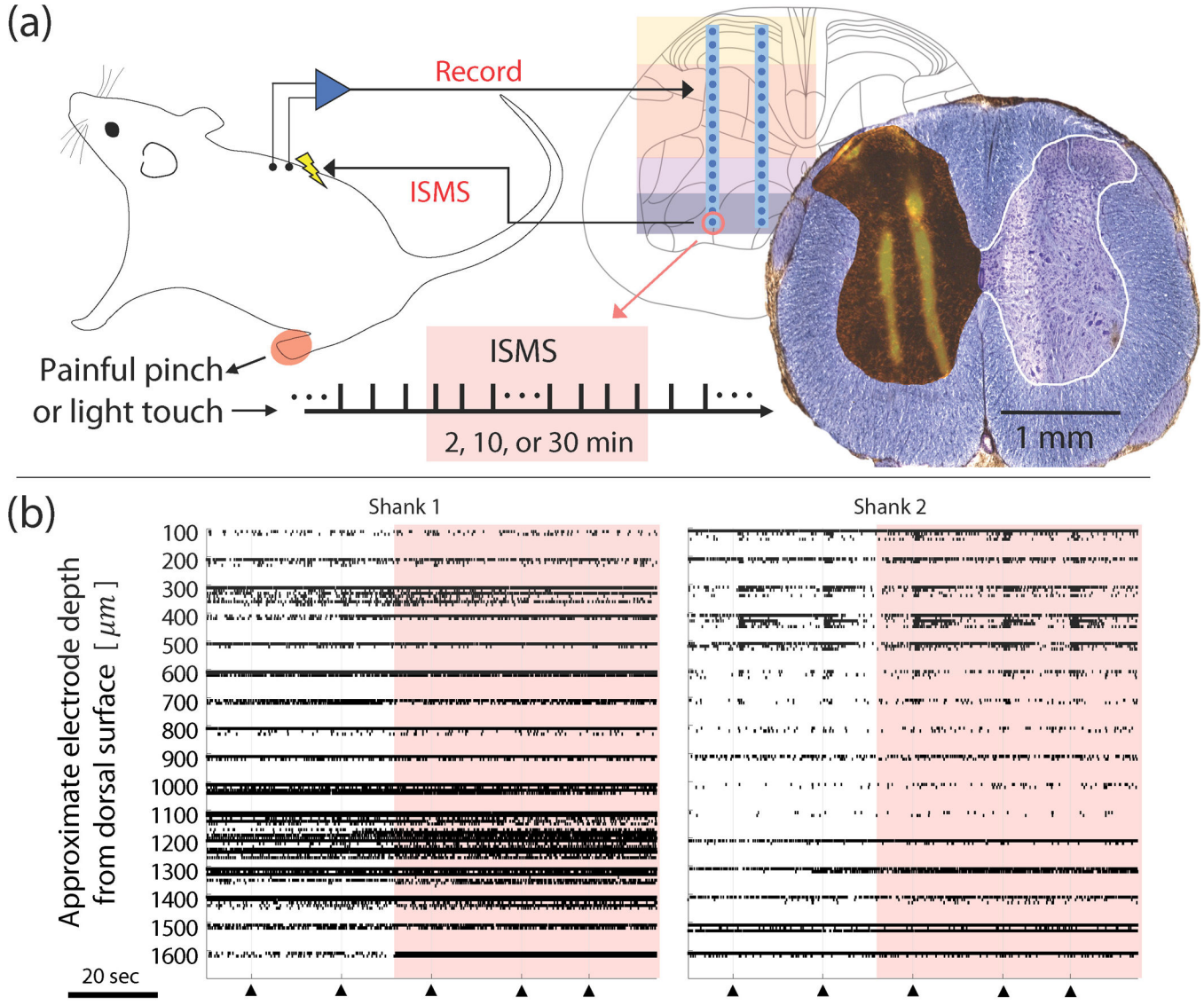

Figure 1.

Overview of experimental setup. (a) Dual-shank, 32 channel microelectrode arrays were implanted into the lumbar enlargement perpendicular to the midline. Electrode coverage area spanned both sensory and motor-dominant regions of the gray matter. Colored portions of the spinal cord schematic illustrate specific regions of the gray matter. From top to bottom: superficial dorsal horn, deep dorsal horn, intermediate gray, and ventral horn. Sub-motor threshold ISMS was delivered on a single channel (circled in red) located in the motor pools before, during, and after mechanical stimulation of the plantar surface of the ipsilateral hindpaw. Right: composite histological image revealing the fluorescent-labeled microelectrode tracks overlayed on the corresponding spinal section (counterstained for myelin and neuron cell bodies). (b) Raster plot illustrating single neuron spike trains discriminated from multi-unit neural data during a trial with painful pinches of the ipsilateral hindpaw (arrowheads) and ISMS (pink shaded region). Note also the high degree of spontaneous neural transmission between pinches.

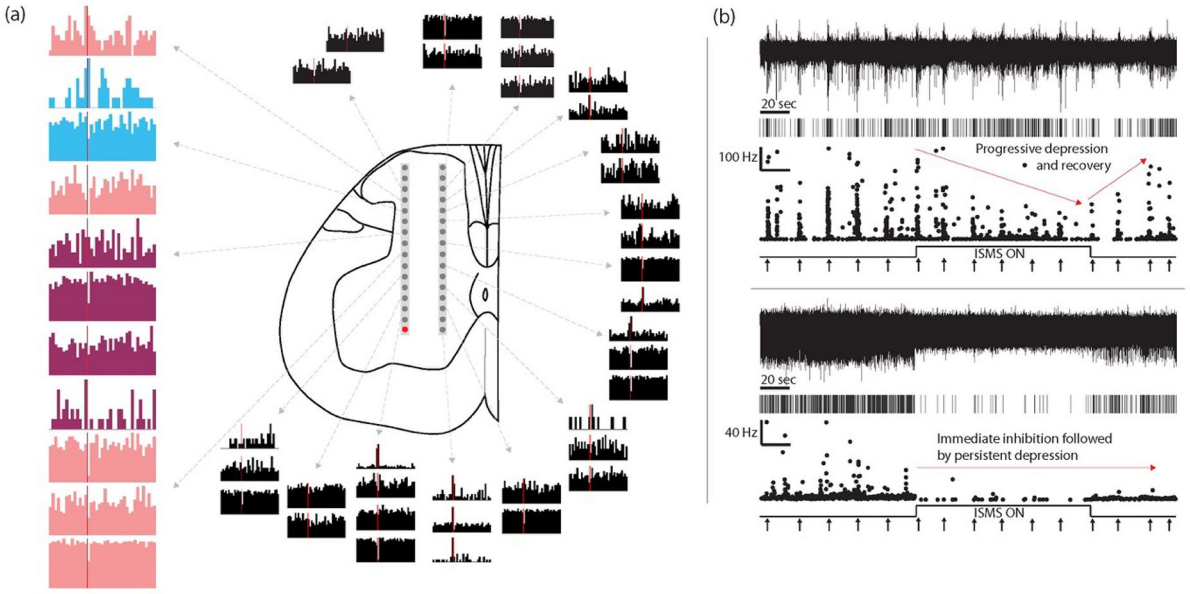

Figure 2.

Sub-motor-threshold ISMS results in widespread modulation of sensorimotor neural transmission. (a) Peristimulus time histograms (PSTH) of single neuron spike trains during 10 min of ISMS (delivered to the red electrode). Vertical red lines depict ISMS pulse onset. All plots depict 50 msec before ISMS and 100 msec after each ISMS pulse. Short-latency actions of ISMS are evident even in superficial regions of the dorsal horn. Colored PSTH plots (left) are neurons determined to be nociceptive specific (NS) or wide dynamic range (WDR). Light blue: NS neuron that exhibited a firing rate increase during painful pinches after ISMS relative to pre-ISMS; light pink: WDR neurons that exhibited firing rate increases during painful pinch after ISMS relative to pre-ISMS; dark magenta: WDR neurons that exhibited firing rate decreases during painful pinch after ISMS relative to pre-ISMS. (b) Representative examples of the depressive effects of ISMS on two WDR neurons during painful pinch. For both subplots: top row, multi-unit neural data from a given electrode; second row, raster plot of spike times for an individual WDR neuron discriminated from the corresponding multi-unit data above; third row, instantaneous firing frequency of the WDR neuron; fourth row, TTL signal indicates periods of ISMS and arrows indicate time of pinches. Note that while ISMS reduces the responsiveness of both neurons to nociceptive transmission, the response patterns themselves are distinct.

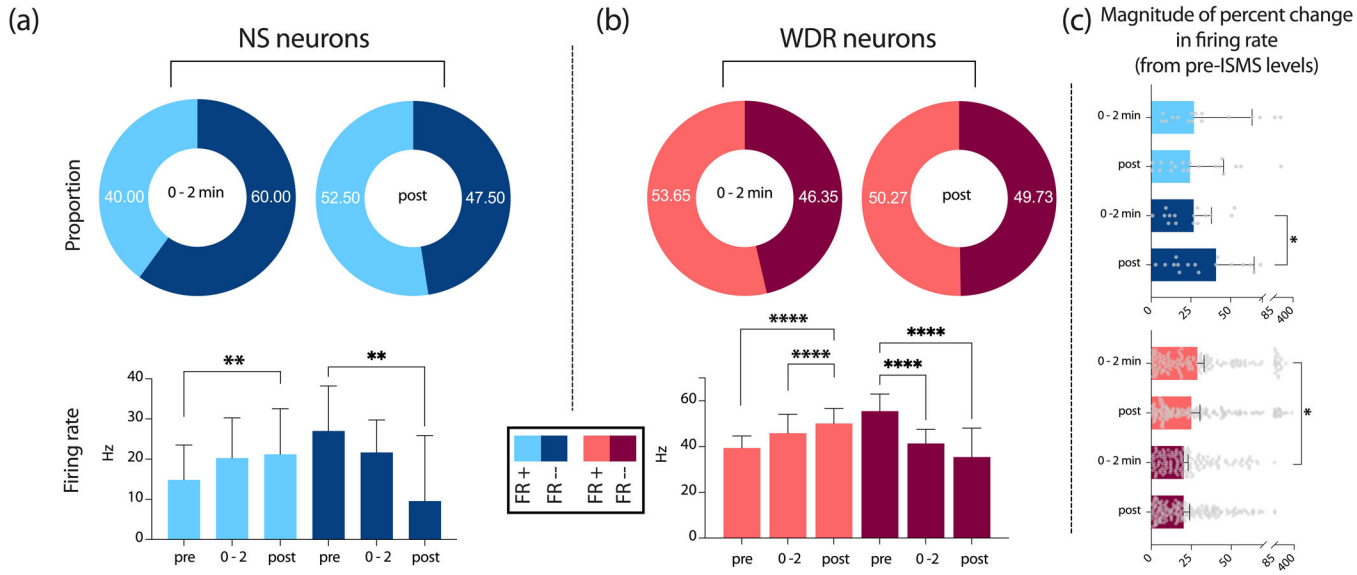

Figure 3.

Changes in firing dynamics associated with 2 min of ISMS. (a) Nociceptive specific (NS) neurons; (b) wide dynamic range (WDR) neurons; (c) magnitude of percent change in firing rate for NS and WDR neurons. Note that darker colors correspond to percent decrease, but are depicted as absolute values to aid comparisons with lighter colors depicting percent increases. (a, b) Donut plots indicate the proportion of neurons exhibiting firing rate increases (lighter color; FR+) or decreases (darker color; FR−) during painful pinches of the ipsilateral hindpaw after 2min of ISMS relative to before ISMS. (a-c) all bar plots depict median ± 95% confidence interval. *p<0.05; **p<0.01; ***p<0.001; ****p<0.0001.

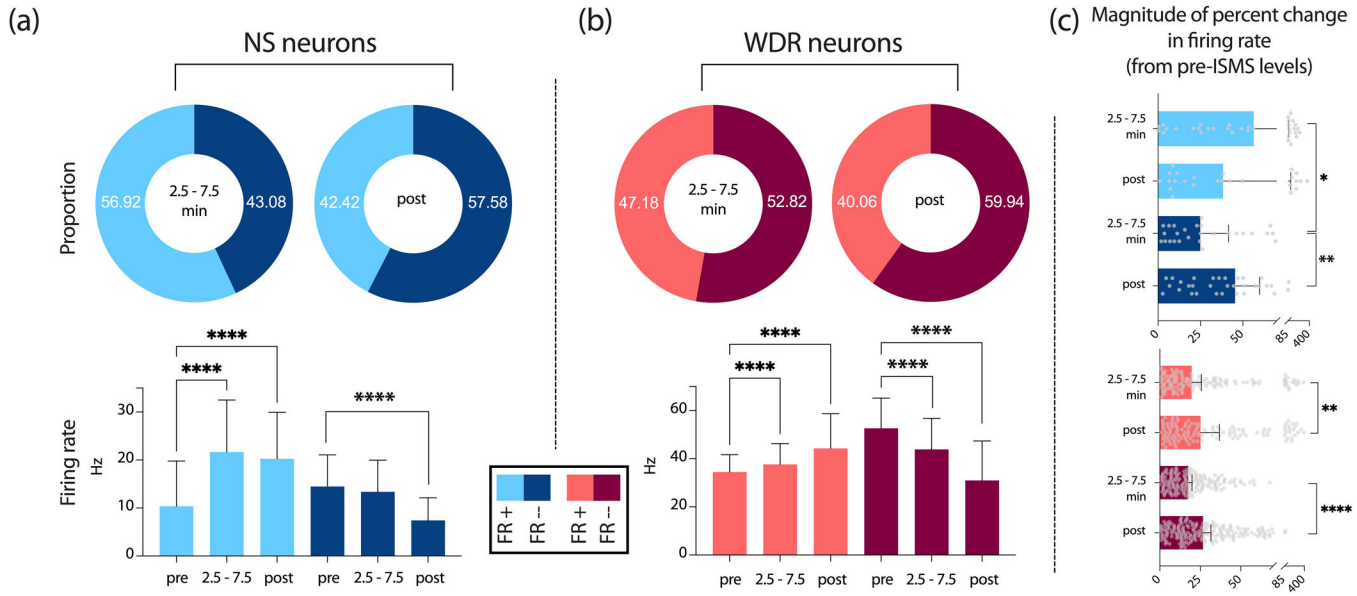

Figure 4.

Changes in firing dynamics associated with 10 min of ISMS. (a) Nociceptive specific (NS) neurons; (b) wide dynamic range (WDR) neurons; (c) magnitude of percent change in firing rate for NS and WDR neurons. Note that darker colors correspond to percent decrease, but are depicted as absolute values to aid comparisons with lighter colors and corresponding percent increases. (a, b) Donut plots indicate the proportion of neurons exhibiting firing rate increases (lighter color; FR+) or decreases (darker color; FR−) during painful pinches of the ipsilateral hindpaw after 2min of ISMS relative to before ISMS. (a-c) all bar plots depict median ± 95% confidence interval. *p<0.05; **p<0.01; ***p<0.001; ****p<0.0001.

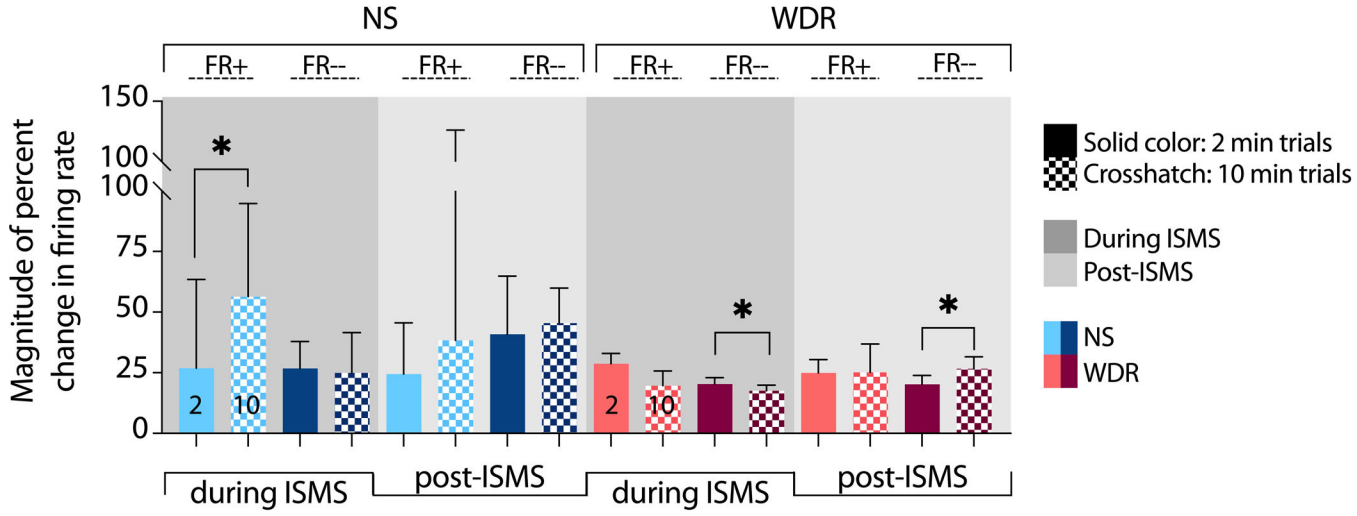

Figure 5.

Comparison of responses to trials of 2 min and trials of 10 min ISMS. Blue colors: Nociceptive specific (NS) neurons; Pink/burgundy colors: wide dynamic range (WDR) neurons. Solid bars: 2 min trials; crosshatched bars: 10 min trials. Darker gray background: comparisons of responses during ISMS of each duration; lighter gray background: comparisons of responses after ISMS. FR+: populations of neurons exhibiting increased firing rates after ISMS compared to before ISMS; FR−: population of neurons exhibiting decreased firing rates after ISMS compared to before ISMS. All bar plots depict median ± 95% confidence interval. *p<0.05.

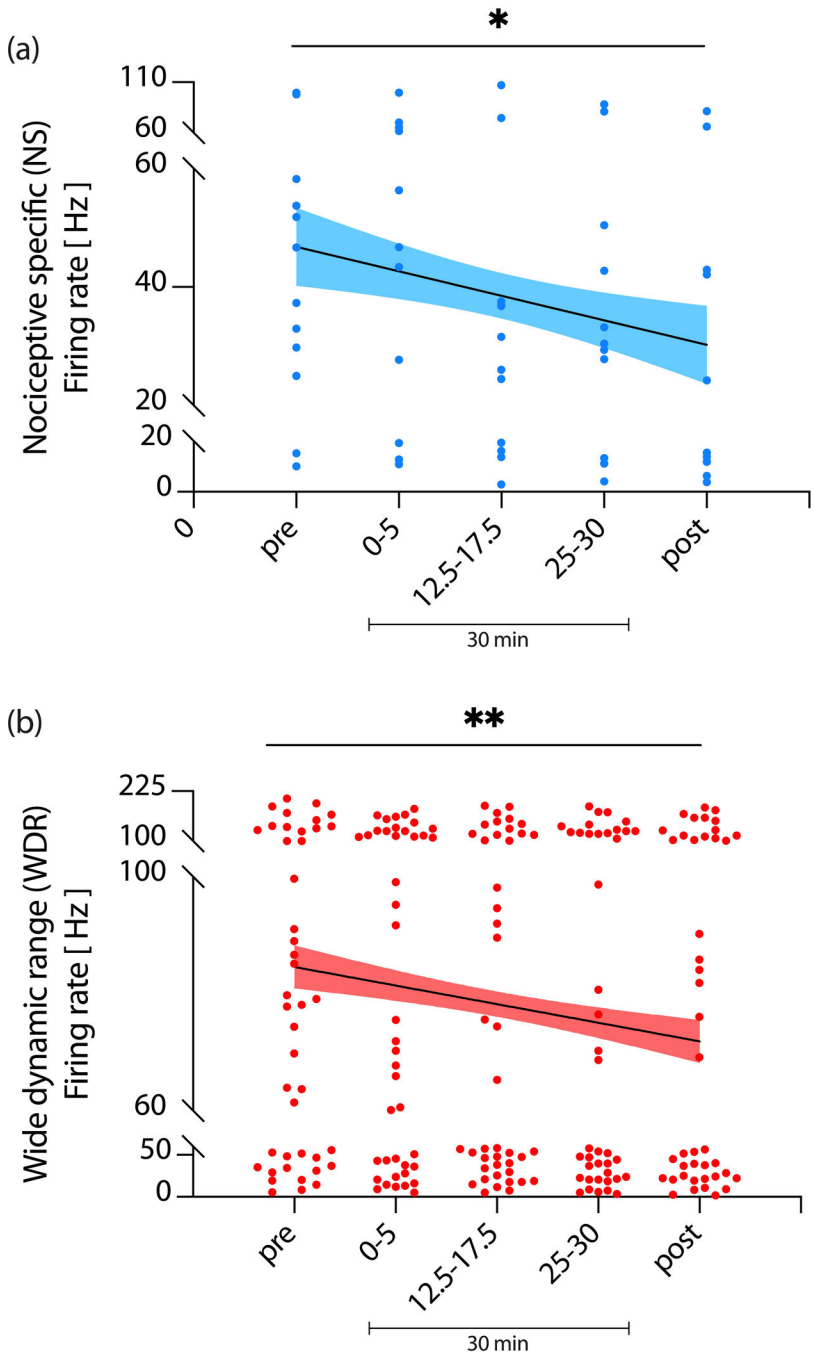

Figure 6.

Firing rate of NS and WDR neurons during induced nociceptive transmission progressively decreases with increasing ISMS duration. (a) NS neurons; (b) WDR neurons; (a, b) y-axis: peak firing rate during painful pinch of the ipsilateral hindpaw; x-axis: timepoint relative to ISMS. ‘During 01’: mean firing rate during the first 5 min of ISMS; ‘during 02’: mean firing rate from 12.5–17.5 min of ISMS; ‘during 03’: mean firing rate from 25–30 min of ISMS. Linear regression fits are shown with 95% confidence bounds. Note that all NS and WDR neurons in their respective pools are included the regression models; i.e., neurons were not

stratified by those that ultimately exhibited firing rate increases vs. decreases post-ISMS. *p<0.05; **p<0.01.

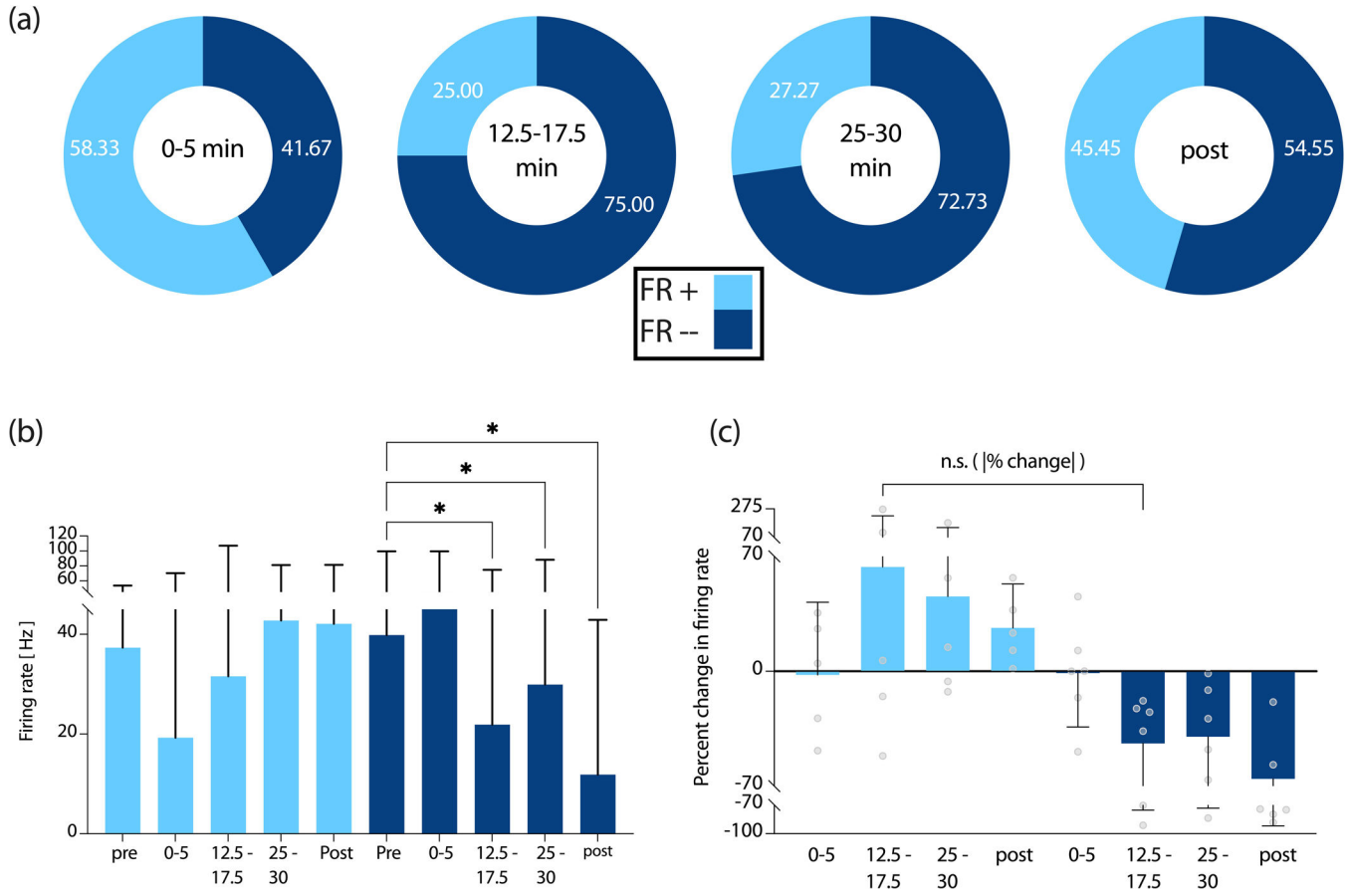

Figure 7.

Changes in NS firing dynamics associated with 30 min of ISMS. (a-c) NS neurons exhibiting firing rate increases (lighter color; FR+) or decreases (darker color; FR−) during painful pinches of the ipsilateral hindpaw after 30 min of ISMS relative to before ISMS. 'During 01': mean firing rate during the first 5 min of ISMS; 'during 02': mean firing rate from 12.5–17.5 min of ISMS; 'during 03': mean firing rate from 25–30 min of ISMS. (a) Donut plots indicate the proportion of NS neurons with increased or decreased firing rates at a given timepoint; (b) peak firing rate of NS neurons at each timepoint during painful pinches of the ipsilateral hindpaw; (c) percent change in firing rate from timepoint indicated to pre-ISMS firing rate during painful pinches of the ipsilateral hindpaw; (b,c) error bars depict 95% confidence interval. *p<0.05; n.s., non-significant.

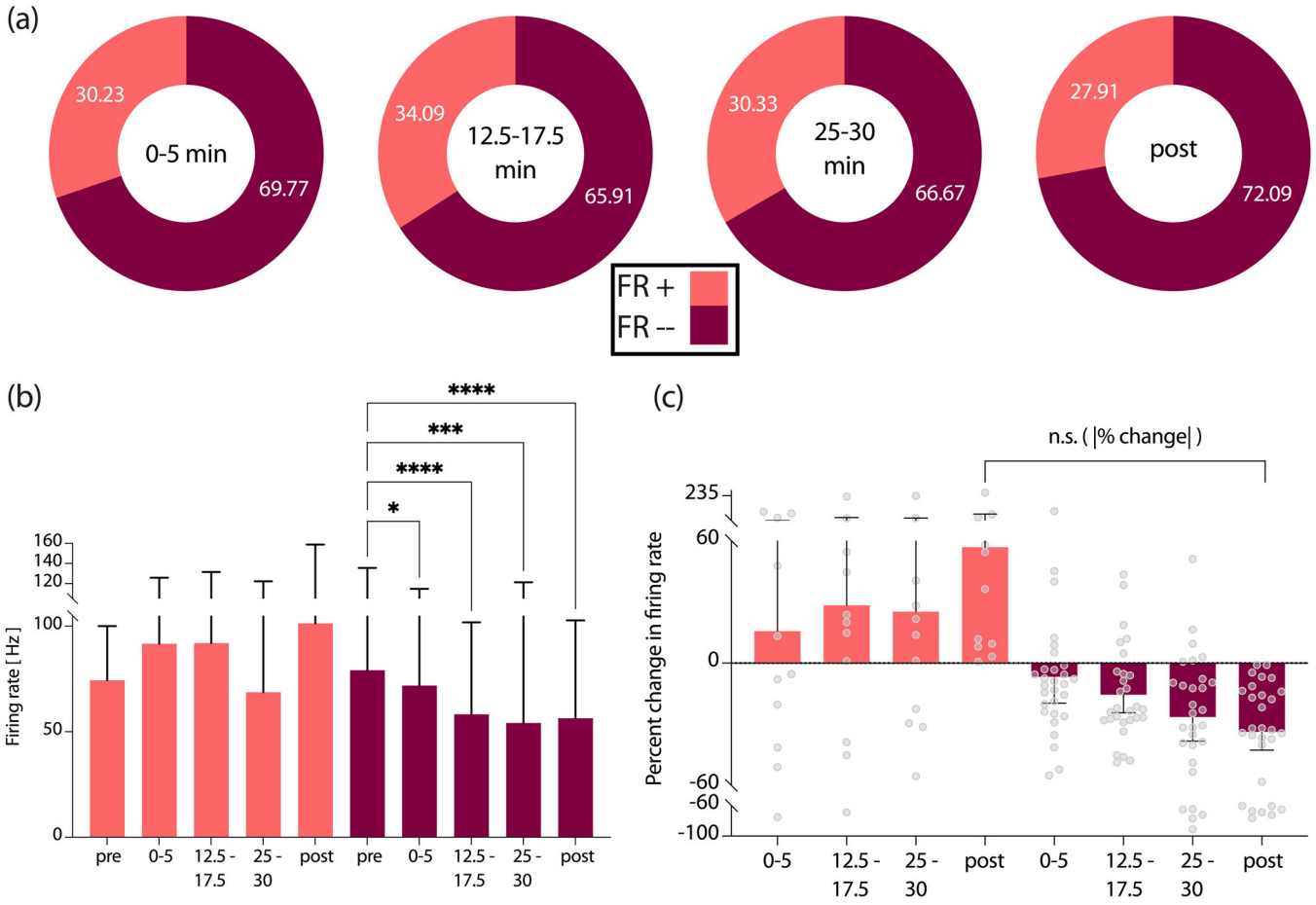

Figure 8.

Changes in WDR firing dynamics associated with 30 min of ISMS. (a-c) WDR neurons exhibiting firing rate increases (lighter color; FR+) or decreases (darker color; FR−) during painful pinches of the ipsilateral hindpaw after 30 min of ISMS relative to before ISMS. 'During 01': mean firing rate during the first 5 min of ISMS; 'during 02': mean firing rate from 12.5–17.5 min of ISMS; 'during 03': mean firing rate from 25–30 min of ISMS. (a) Donut plots indicate the proportion of WDR neurons with increased or decreased firing rates at a given timepoint; (b) peak firing rate of WDR neurons at each timepoint during painful pinches of the ipsilateral hindpaw; (c) percent change in firing rate from timepoint indicated to pre-ISMS firing rate during painful pinches of the ipsilateral hindpaw; (b,c) error bars depict 95% confidence interval. *p<0.05; **p<0.01; ***p<0.001; ****p<0.0001; n.s., non-significant.

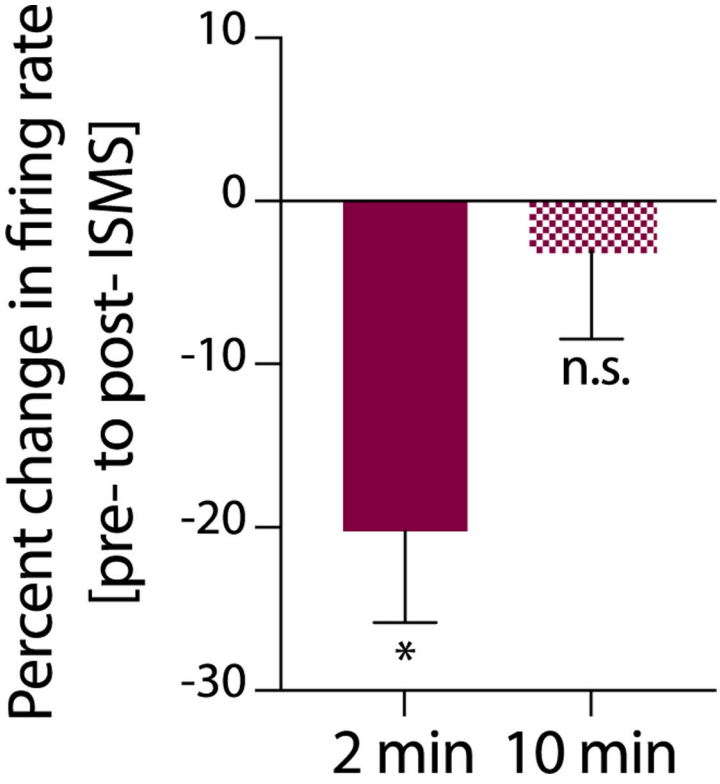

Figure 9.

ISMS-induced effects on WDR responses to non-nociceptive cutaneous feedback. Bar height reflects the median precent change in firing rate of the pool of all identified WDR neurons during light touches of the L5 dermatome after a given duration of motor-targeted ISMS. Solid bar: change in firing rate during light touch at the conclusion of 2 min of ISMS (relative to pre-ISMS); crosshatched bar: percent change in firing rate during light touch at the conclusion of 10 min of ISMS. *p<0.05